

MINERALOGIA, 39, No. 1–2: 7–30 (2008)

DOI: 10.2478/v10002-008-0002-8

www.Mineralogia.pl

MINERALOGICAL SOCIETY OF POLAND

POLSKIE TOWARZYSTWO MINERALOGICZNE



Original paper

Whole rock major element influences on monazite growth: examples from igneous and metamorphic rocks in the Menderes Massif, western Turkey

Elizabeth J. CATLOS¹ *, Courteney B. BAKER², Ibrahim ÇEMEN², Cenk OZERDEM³

¹ The University of Texas at Austin, Jackson School of Geosciences, 1 University Station C1100, Austin, TX 78712-0254, USA; e-mail: ejcatlos@gmail.com

² Oklahoma State University, School of Geology, 105 Noble Research Center, Stillwater, OK, 74075, USA; e-mail: b.baker@okstate.edu, ibrahim.cemen@okstate.edu

³ GAMA Qatar, Almana Building 6th Floor, Airport Road, P.O. Box 22825, Doha, Qatar; e-mail: cenkozerdem@yahoo.com

* Corresponding author

Received: August 11, 2007

Accepted: April 05, 2008

Abstract. Monazite (LREEPO₄) is a radiogenic, rare-earth bearing mineral commonly used for geochronology. Here we examine the control of major element chemistry in influencing the crystallization of monazite in granites (Salihli and Turgutlu bodies) and garnet-bearing metamorphic assemblages (Bozdag and Bayindir nappes) from the Menderes Massif, western Turkey. In S-type granites from the massif, the presence of monazite correlates to the CaO and Al₂O₃ content of the whole rock. Granites with monazite only are low Ca (0.6–1.8 wt% CaO). As CaO increases (from 2.1–4.6 wt%), allanite [(Ce,Ca,Y)₂(Al,Fe³⁺)₃(SiO₄)₃(OH)] is present. Higher Al₂O₃ (>15 wt%) rocks contain allanite and/or monazite, whereas those with lower Al₂O₃ contain monazite only. However, examining data reported elsewhere for A-type granites, the correlation between major element chemistry and presence of monazite is likely restricted to S-type lithologies. Pelitic schists of the Menderes Massif show no correlation between major element chemistry and presence of monazite. One Bayindir nappe sample contains both prograde garnets and those affected significantly by diffusion. These rocks have likely experienced a complicated multi-stage tectonic history, which influenced their current mineral assemblages. The presence of monazite in a metamorphic rock can be influenced by the number, duration, and nature of events that were experienced and the degree to which fluids were involved. The source of monazite in the Bayindir and Bozdag samples was likely reactions that involved allanite. These reactions may not have significantly changed the bulk composition of the rock.

Key-words: monazite, extensional tectonics, geochemistry, geochronology

1. Introduction

Due to its stability over a wide range of pressure-temperature (P-T) conditions, mineral assemblages, and whole rock concentrations, monazite (LREEPO₄) is an important mineral for geochronology. The mineral is found most commonly in alkaline and peralkaline plutons (e.g., Schärer and Allègre 1983; Montero et al. 1988; Kovalenko et al. 1995; Conceicao 2000; Dostal et al. 2004; Xie et al. 2006). Although rarely reported, monazite can also exist in basalts (e.g., Hlava 1974), notably on the Moon (Lovering et al. 1974; Kartashov et al. 2006). Monazite is an economically important constituent of carbonatites (e.g., Viladkar 1998; Kim et al. 2005; Kanazawa and Kamitani 2006) often as a late stage mineral (Wall and Mariano 1996). In metamorphic lithologies, monazite is often reported in rocks that have experienced conditions coincident with the garnet isograd (Smith and Barreiro 1990) or clinopyroxene isograd (Bingen et al. 1996), but the mineral can also exist from very low (<270–300°C; e.g., Krenn and Finger 2007; Rasmussen et al. 2007; Janots et al. 2007) to ultra-high temperatures (>900°C; Santosh et al. 2006; Suzuki et al. 2006).

Monazite is common in sediments and sedimentary rocks (e.g., Kapoor et al. 1977; Chen et al. 2006; Yang et al. 2006) as evidenced by radioactive monazite sands that pose health hazards in India (e.g., Jaikrishan et al. 1999), Turkey (Örgün et al. 2007), and Brazil (deMoura et al. 2002). Although mineral stability in sediments is dependent on a number of factors (e.g., Milliken 2007), monazite has been found to be more stable than staurolite or chlorite in sandstones (Barakat et al. 1993). Detrital monazite provides valuable information regarding provenance, as it can be dated, is compositionally variable, and forms in a variety of lithologies (e.g., Morton and Hallsworth 1994; Evans et al. 2001; Kusiak et al. 2006; Yang et al. 2006).

Monazite has long been thought to be unstable in pelitic schists during diagenesis (e.g., Overstreet 1967; Smith and Barreiro 1990; Akers et al. 1993; Kingsbury et al. 1993; Harrison et al. 1997). Monazite has been said to be “essentially unknown in low-grade pelitic rocks that contain detrital zircon” (Akers et al. 1993) and “will break down” during low-grade metamorphism of pelites (Overstreet 1967; Kingsbury et al. 1993). However, diagenetic/ authigenic monazite has been reported in the Welsh Basin, UK (Evans and Zalasiewicz 1996; Lev et al. 1998; 1999; 2000; Evans et al. 2002; Wilby et al. 2007), the Shisanlitai Formation of Liaoning Province, China (Song 1999), the Soanesville Group, Pilbara Craton, NW Australia (Rasmussen et al. 2007), and the lower Belt-Purcell Supergroup in western North America (González-Álvarez et al. 2006). Experiments with synthetic monazite suggest the mineral can found to be stable at <250°C (Janots et al. 2007).

Monazite ages from metamorphic and igneous rocks are often vital pieces of information about the tectonic history of areas that serve as examples for plate tectonic processes. For example, Pliocene monazite grains from the Main Central Thrust zone in the Himalayas constrain models for the evolution of the range (Harrison et al. 1997; Catlos et al. 2001). Monazite from several major shear zones in the Alps formed at disparate times, helping to constrain episodic movement or fluid flow within the structures (e.g., Vavra and Schaltegger 1999; Hermann and Rubatto 2003). Monazite ages of granites located in the Carpathians lend important insight into complicated tectonic and magmatic history of the region (e.g., Finger and Broska, 1999; Finger et al. 2003). Monazite is dated to time compression (e.g., Harrison et al. 1998; Claesson et al. 2001; Catlos et al. 2001; Dahl et al. 2005), extension (e.g., Gilotti and

McClelland 2005; Catlos and Çemen 2005; Kaur et al. 2006), even strike-slip events (e.g., Schärer et al. 1994; 1996; Gilley et al. 2003; Murphy and Copeland 2005).

In recent years, monazite dating has proliferated perhaps due to developments in a variety of techniques and instrumentations (Fig. 1). Many researchers have discussed which tool is best to use, whether it be an ion microprobe (e.g., DeWolf et al., 1993; Harrison et al. 1995; Grove and Harrison 1999), electron microprobe (e.g., Suzuki et al. 1991; Montel et al. 1996; Williams et al. 1999; Jercinovic and Williams 2005; Pyle et al. 2005; Williams et al. 2007), or laser-based mass spectrometry (e.g. Machado and Gauthier 1996; Poitrasson et al. 1996; Simonetti et al. 2006). Particle-induced X-ray emission (PIXE, e.g., Martin 1980) has also been applied to monazite geochronology (e.g., Bruhn et al. 1999; Mazzoli et al. 2002; Lekki et al. 2003; Vaggelli et al. 2006; Kusiak and Lekki 2008). Aliquots of monazite separated from rocks have long been dated using conventional thermal ionization mass spectrometry methods (e.g., Tilton and Nicolaysen 1957; Schärer and Allègre 1983).

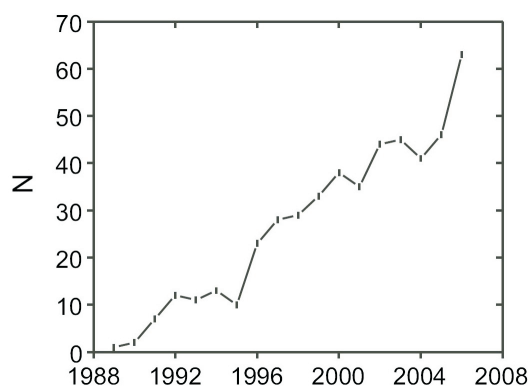


Fig. 1. Number of papers referencing “monazite and geochronology” from the years 1988 to 2006. Informal analysis done using ISI Web of Science, Thompson Scientific

In this paper, we seek to evaluate a common question that arises regarding the paragenesis of monazite to aid those using the mineral in their pursuit to address geologically important problems. This is: does a rock’s major element chemical composition (i.e., CaO, Al₂O₃, Fe₂O₃) control the presence of monazite in igneous and metamorphic assemblages? This apparently simple question requires answers prior to linking monazite ages to tectonic events or using the mineral to ascertain rates. To help answer this question, we obtained geochemical data from metamorphic and igneous assemblages of the Menderes Massif in western Turkey.

2. Geologic background of the Menderes Massif

The Menderes Massif is one of several Aegean metamorphic core complexes (Fig. 2). Understanding the geochronologic and thermobarometric history of its rocks provides information about the large-scale geodynamic processes that facilitate extension in the Earth’s lithosphere. The region experienced a set of tectonic events, including compression during the Cambro-Ordovician and Eocene, followed by large-scale extension during the Oligocene

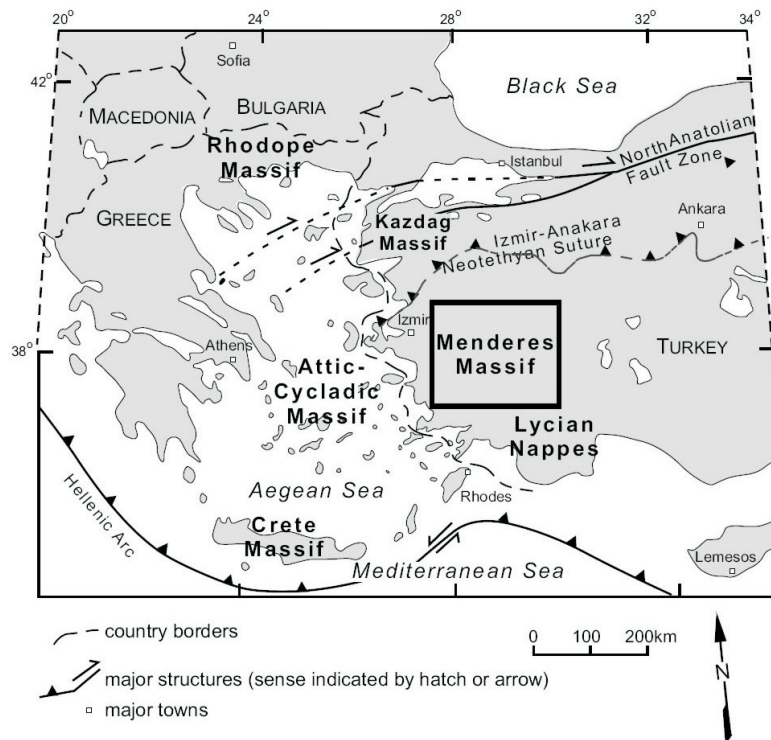


Fig. 2. Simplified map of the Aegean region showing the location of major structures and massifs.
Figure 3 shows a more detailed map of the Menderes Massif

(see Çemen et al. 2006). Monazite ages reported from the massif range from the Pan African to the Pliocene (Catlos and Çemen 2005). Because of its multi-stage tectonic history and exposure of a wide variety of metamorphic and igneous rocks, the region is ideal for testing ideas about monazite paragenesis.

The massif is divided into northern (Gördes), central, and southern (Çine) sections based on the presence of E-W trending grabens, northern Gediz (Alasehir), central Küçük Menderes, and southern Büyük Menderes (see review by Bozkurt and Oberhaensli 2001) (Fig. 3). Metamorphic rocks are further divided into a series of nappes, exposed via warping, exhumation, and/or extension (Dora et al. 2001; Gessner et al. 2001; Ring et al. 2001; 2004; Regnier et al. 2007). The Bayindir nappe is structurally lowest, and consists of shelf sediments metamorphosed to lower greenschist facies during the Cenozoic (Gessner et al. 2001). In the overlying Çine and Bozdag nappes, Precambrian deformation and metamorphism are evident from eclogites (600–650 Ma), migmatites (540–550 Ma), and post-deformational plutons (540–560 Ma) (e.g., Satir and Friedrichsen 1986; Loos and Reischmann 1999; Gessner et al. 2004). The Çine nappe is comprised of amphibolite to granulite facies ortho- and paragneisses intercalated with metabasite (Gessner et al. 2001; Sengun et al. 2006), whereas the Bozdag nappe is characterized by amphibolite-facies garnet-mica schists. These units are interpreted as Pan-African in origin, but with a Cenozoic greenschist (Gessner et al. 2001) to amphibolite-grade metamorphic overprint (Catlos and Çemen 2005).

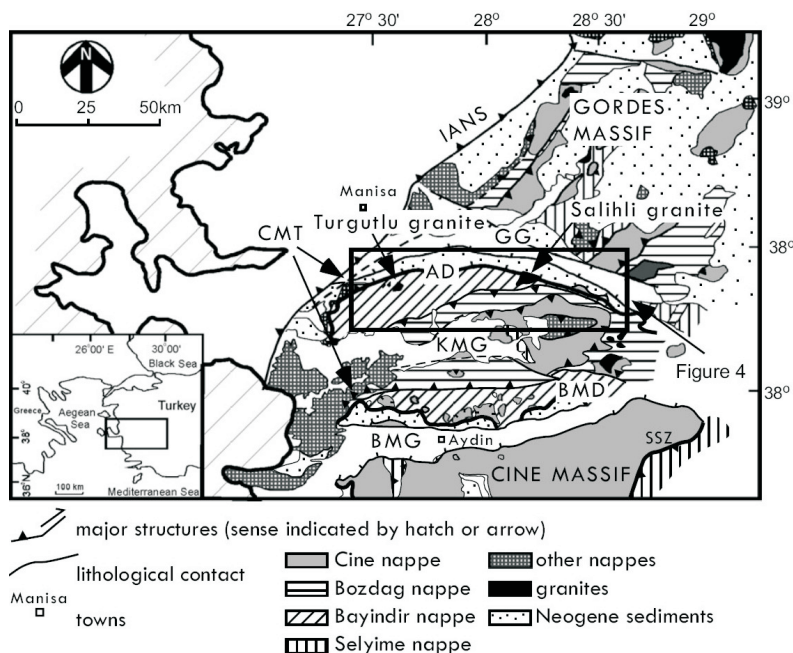


Fig. 3. Map of the Menderes Massif after Sözbilir (2001) and Gessner et al. (2001). Inset shows the location of the massif in relation to western Turkey. See Figure 4 for sample locations. Abbreviations: GG, Gediz Graben; AD, Alasehir detachment; KMG, Küçük Menderes Graben; BMG, Büyük Menderes Graben; CMT, Cyclades Menderes Thrust

This study focuses on rocks collected along the central Menderes Massif's north-dipping Alasehir detachment (Figs. 3 and 4). The structure is located along the northern margin of central Menderes metamorphic core complex and exposes garnet-bearing schists and gneisses of the Bayindir and Bozdag nappes intruded by the Salihli and Turgutlu granites (Hetzl et al. 1995a; Glodny and Hetzel 2007). The granites that intrude the detachment are separated by an E-W distance of ~50 km and were likely affected by low- to mid-greenschist facies conditions during ductile deformation during the Late Miocene (Hetzl et al. 1995a, 1995b; Isik et al. 2003; Glodny and Hetzel 2007).

3. Sample collection and mineral assemblages

Samples EB01, EB02, EB03, EB05, and CC20 were collected from the Salihli granite and samples EB06, EB08A, EB08B, EB09A, and EB09B were collected from the Turgutlu granite (Table 1; Fig. 4). Overall, the Salihli samples contain $Qtz + Pl + Kfs + Bt + Ap + Zrn \pm Ilm \pm Chl \pm Ms \pm Px \pm Aln \pm Ep \pm Xtm \pm Mnz \pm Th \pm Ttn \pm Rt \pm Hem \pm Clt \pm Htn$ (abbreviations after Kretz 1983). Only Salihli sample CC20 has monazite. Chloritoid was found in Salihli samples CC20 and EB05. Turgutlu samples contain $Qtz + Pl + Kfs + Bt + Ms + Ap + Mnz + Zrn \pm Chl + Ilm + Xtm \pm Aln \pm Rt \pm Ttn \pm Sil \pm Hem$. Fibrous sillimanite was found only in Turgutlu sample EB09B. All granites analyzed are S-type, subalkalic, and peraluminous. All Salihli samples are

granodiorites, except CC20, which is a leucogranite. Turgutlu rocks can be classified on the basis of their chemistry as granodiorites, monzogranites, or syenogranites. For simplification, we refer to them as “granites.” All Salihli samples contain allanite, except CC20A, which contains monazite.

Several garnet-bearing rocks (sample numbers have MM abbreviations) were collected from the Bayindir and Bozdag nappe located in close proximity to the Salihli granite (Table 1; Fig. 4). These samples contain $Grt + Qtz + Ms \pm Bt \pm Pl \pm Mnz \pm Rt \pm Chl \pm Ap \pm Ilm \pm Tur \pm Zr \pm Aln \pm Py \pm Xtm \pm St \pm Hem \pm Th \pm Gr$. Bozdag samples (MM26 and MM28) differ from Bayindir rocks in that they have staurolite.

TABLE 1

Mineral assemblages	
Sample	Mineral assemblage*
Salihli granitic samples**	
EB01	Ilm + Chl + Ms + Px + Aln + Ep + Ttn + Hem
EB02	Ilm + Chl + Ms + Px + Aln + Ep + Ttn
EB03	Ilm + Chl + Ms + Px + Aln + Ep + Ttn
EB05	Chl + Aln + Ep + Ttn + Cld
CC20	Ilm + Ms + Cld + Xtm + Mnz + Rt + Th
Turgutlu granitic samples**	
EB06	Ilm + Ms + Aln + Xtm + Mnz + Rt + Htn
EB08A	Ilm + Chl + Ms + Xtm + Mnz + Rt
EB08B	Ilm + Chl + Ms + Aln + Mnz + Rt
EB09A	Ilm + Chl + Ms + Xtm + Mnz + Ttn + Hem
EB09B	Ilm + Ms + Sil + Xtm + Mnz + Hem
Bayindir Nappe garnet bearing assemblages***	
MM45	Bt + Pl + Mnz + Rt + Chl
MM48	Bt + Pl + Mnz + Rt + Chl + Ap + Ilm
MM33	Bt + Pl + Mnz + Rt + Chl + Ap + Tur
MM36	Bt + Pl + Mnz + Rt + Chl + Ilm + Zr + Aln
MM39	Bt + Pl + Mnz + Rt + Chl + Ap + Ilm + Zr + Aln + Py
MM40	Bt + Pl + Mnz + Rt + Chl + Ap + Ilm + Zr + Aln + Py + Gr
MM41	Bt + Pl + Mnz + Rt + Chl + Ilm + Zr + Py + Xtm
MM32	Bt + Pl + Mnz + Rt + Chl + Tur
Bozdag Nappe garnet bearing assemblages***	
MM26	Bt + St + Mnz + Rt + Ap + Ilm + Zr + Gr + Hem + Th
MM28	St + Mnz + Rt + Ap + Ilm + Zr + Gr + Hem

* Mineral abbreviations after Kretz (1983).

** All Salihli and Turgutlu samples contain $Qtz + Pl + Kfs + Bt + Ap + Zrn$.

*** All Bayindir and Bozdag nappes samples contain $Grt + Qtz + Ms$.

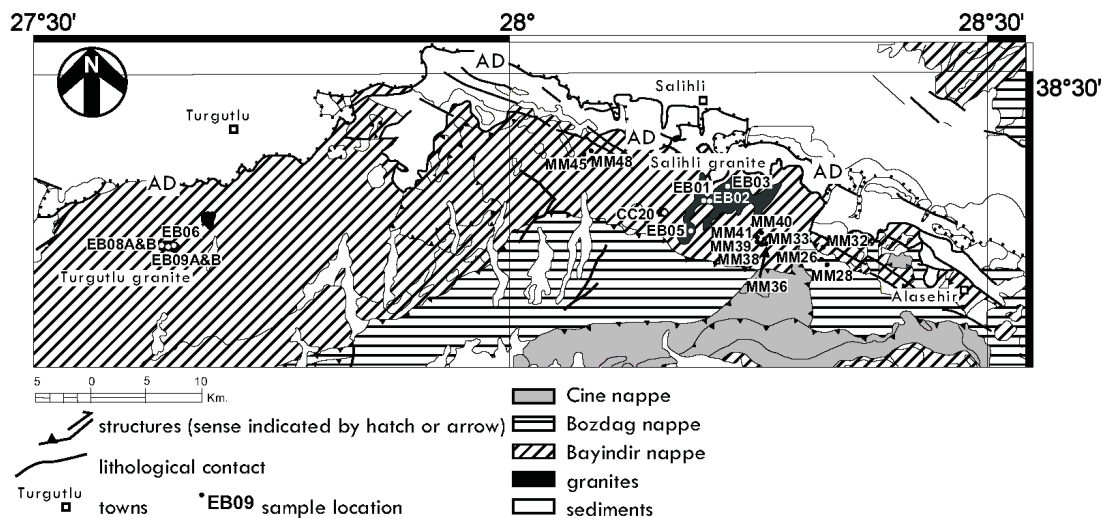


Fig. 4. Geologic and sample location map modified after Konak (2002), Seyitoglu et al. (2002), Isik et al. (2003), and our observations. Abbreviations: AD, Alasehir detachment. EB and CC samples were collected from the granites, whereas MM samples are garnet-bearing metamorphic assemblages

All samples were imaged using backscattered electrons (BSE) and some monazite grains were X-ray element mapped (Y, U, Th, Ca) using an electron microprobe. Operating conditions for the element maps were a probe current of 120–200 nA, beam size of ~2 μm , and count-times of ~30–35 ms. Operating conditions for imaging and compositional analyses were an accelerating voltage of 15 kV and a beam current of ~20 nA. Whole rock fusion ICP analyses were obtained from all metamorphic rocks and granites in this study from Activation Laboratories; compositions are reported in Tables 2–4. Detection limits are 0.01% for all major elements, except MnO and TiO₂, which are 0.001%. Reported analytical uncertainties are better than $\pm 1\%$.

4. Monazite and whole rock compositions

As monazite is found in a wide variety of igneous and metamorphic rocks, several researchers have questioned if the presence of the mineral could be based on the rock's bulk composition. In granites, monazite has been reported to form at low Ca activity, whereas allanite, a radiogenic rare-earth epidote-group mineral, precipitates at higher Ca levels (e.g., Lee and Dodge 1964; Cuney and Friedrich, 1987; Broska and Siman 1998; Broska et al. 2000). Monazite may be more typical of S-type, Ca-poor or peraluminous granitoids than in I-type lithologies (see Snetsinger 1967; Parrish 1990; Broska and Siman 1998; Meyer et al. 1994). To ascertain if monazite is unstable at specific CaO wt% levels (i.e., 1.4–1.8 wt%, Lee and Dodge 1964; Lisitsina et al. 1965; Cuney and Friedrich 1987), we obtained geochemical data from the Salihli and Turgutlu granites exposed in western Turkey (Tables 2 and 3; also Glodny and Hetzel 2007).

We include backscattered electron (BSE) images of allanite from the Salihli and Turgutlu granites in Fig. 5. Turgutlu allanite grains are typically anhedral with diffuse boundaries, filling cracks or crystal faces within other minerals, typically K-feldspar (Fig. 5). In contrast, Salihli

TABLE 2

Major element compositional data from the salihli granite (western Turkey) that contain allanite as the main lree accessory phase*

	EB01**	EB01	EB01	EB02	EB02	EB03	EB05	EB05	EB05
SiO ₂	67.72	66.16	67.32	65.86	66.54	65.25	69.24	68.64	68.12
Al ₂ O ₃	15.79	16.11	16.38	16.69	16.59	16.08	15.52	15.77	16.09
Fe ₂ O ₃ (T)	3.38	3.45	3.81	3.97	3.90	3.61	3.21	3.16	3.27
MnO	0.06	0.07	0.07	0.08	0.07	0.07	0.06	0.06	0.06
MgO	1.39	1.42	1.56	1.69	1.66	1.54	1.18	1.18	1.26
CaO	3.94	4.07	3.77	4.60	4.13	4.31	3.72	3.59	3.80
Na ₂ O	2.95	3.06	2.87	3.13	2.96	3.13	3.03	3.04	3.02
K ₂ O	2.62	2.81	2.73	2.75	2.83	2.71	3.24	3.46	2.95
TiO ₂	0.56	0.56	0.607	0.64	0.614	0.57	0.49	0.49	0.54
P ₂ O ₅	0.16	0.18	0.17	0.20	0.15	0.16	0.13	0.14	0.14
LOI	1.11	1.04	1.25	0.77	0.90	1.56	0.76	0.63	0.90
Total	99.68	98.93	100.5	100.40	100.3	98.98	100.60	100.20	100.2

* Compositions (in wt%) were obtained using whole rock fusion ICP methods.

** In some cases, we include more than one analysis of a sample. See Table 1 for mineral assemblages.

TABLE 3

Major element compositional data from granites from the menderes massif that contain both monazite only and/or allanite + monazite

	Aln + Mnz				Mnz only				
	EB06**	EB06	EB08B	EB08A	EB08A	EB09A	EB09A	EB09B	CC20
SiO ₂	68.01	70.33	70.68	68.48	69.23	74.69	75.35	74.02	75.69
Al ₂ O ₃	15.96	15.67	15.71	14.51	14.76	14.83	14.66	14.90	12.95
Fe ₂ O ₃ (T)	3.19	2.82	2.17	4.29	4.21	1.29	0.74	1.27	1.22
MnO	0.07	0.06	0.06	0.10	0.10	0.02	0.014	0.02	0.02
MgO	1.19	0.75	0.54	1.18	1.18	0.20	0.14	0.20	0.32
CaO	3.75	2.55	2.11	1.01	1.01	0.60	0.73	0.61	1.80
Na ₂ O	3.07	3.43	3.26	2.67	2.64	3.11	3.41	3.06	3.24
K ₂ O	3.67	3.62	4.10	5.40	5.48	4.67	4.64	4.94	2.80
TiO ₂	0.50	0.31	0.22	0.50	0.49	0.11	0.08	0.11	0.13
P ₂ O ₅	0.14	0.11	0.12	0.12	0.1	0.10	0.11	0.11	0.04
LOI	0.58	0.54	0.86	0.69	0.92	1.04	0.64	1.67	1.41
Total	100.10	100.2	99.84	98.95	100.1	100.70	100.50	100.90	99.62

* Compositions (in wt%) were obtained using whole rock fusion ICP methods.

** In some cases, we include more than one analysis of a sample. See Table 1 for mineral assemblages.

TABLE 4

Major element compositional data from metamorphic rocks from the menderes massif

	Aln + Mnz					Mnz only				
	MM40	MM39	MM36	MM33	MM32	MM28	MM26	MM41	MM45	MM48
SiO ₂	54.8	66.7	62.4	62.8	57.5	63.8	64.6	65.8	60.5	65.3
Al ₂ O ₃	17.7	14.9	17.0	15.6	22.3	20.4	19.4	13.6	12.0	15.3
Fe ₂ O ₃	8.51	6.96	7.19	7.30	5.71	9.45	8.67	7.34	4.77	6.75
MnO	0.10	0.08	0.09	0.08	0.08	0.06	0.06	0.09	0.31	0.07
MgO	3.20	2.31	2.69	2.76	1.25	0.65	0.66	2.28	1.94	2.36
CaO	1.68	1.13	1.65	1.56	1.36	0.38	0.29	1.82	7.04	1.06
Na ₂ O	2.37	1.89	2.47	2.46	5.76	0.45	0.71	3.18	1.74	2.27
K ₂ O	3.53	3.03	2.69	2.89	3.11	1.16	1.66	1.71	2.34	2.16
TiO ₂	0.93	0.83	0.89	1.01	0.85	1.21	1.36	1.27	0.57	0.79
P ₂ O ₅	0.28	0.23	0.24	0.29	0.14	0.25	0.11	0.30	0.06	0.24
LOI	5.89	2.41	3.34	1.85	2.14	2.49	2.47	1.49	8.65	2.68
Total	99.0	100.5	100.6	98.6	100.2	100.4	100.0	98.8	99.9	99.0

All oxides obtained using whole rock fusion ICP methods. All are Bozdag nappe samples, except MM26 and MM28.

allanite grains are zoned, euhedral to subhedral, and can be significantly affected by radiation damage. These allanite grains often contain inclusions of other minerals, including zircon, apatite, and quartz. Radiation-damage induced cracks in the Salihli allanite are often filled by re-crystallized material, suggesting the presence of a fluid phase. Recently, 16.1 ± 0.2 Ma U-Pb ages were reported from aliquots of allanite separated from the Salihli granite (Glodny and Hetzel 2007). The BSE images suggest that the precise ages reported for allanite from the Salihli samples should be interpreted with caution.

X-ray element maps (Y, U, Th, Ca) and high resolution BSE images were obtained from monazite grains located in Salihli sample CC20 (Fig. 6) and Turgutlu rocks EB08A (two grains; Fig. 7), and EB08B and EB09A (Fig. 8). Zoning patterns and elemental distributions within monazite have been used to reconstruct stages of geologic and tectonic processes (e.g., Williams and Jercinovic 2002). Mapped monazite grains are located in plagioclase (EB08A, EB09A), biotite (EB08A, CC20), or quartz (EB08B). The Salihli monazite (CC20) has a darker core and lighter rim in BSE, with patches of bright material located around its rim (Fig. 6), whereas Turgutlu monazites show muted, patchy, sector, or oscillatory zoning. The zoning in the BSE images correlates to the grain's distribution of Th (e.g., EB09A, CC20) or U (e.g., EB08B). Turgutlu monazites show similar zoning in U and Y. For example, monazite grains mapped in EB09A, EB08A, and EB08B have low Y and U cores and high Y and U rims. This cannot be generalized to the CC20 Salihli monazite, as this grain has a high Y and low U core and a low Y and high U rim. Some monazite grains have inclusions of apatite (EB08B, EB09A; Fig. 8) or appear to be surrounded by a high Ca phase (CC20, Fig. 6 and EB08A; Fig. 7). The high Ca regions surrounding the monazite in CC20 and EB08A are located near cracks or regions of bright contrast in BSE.

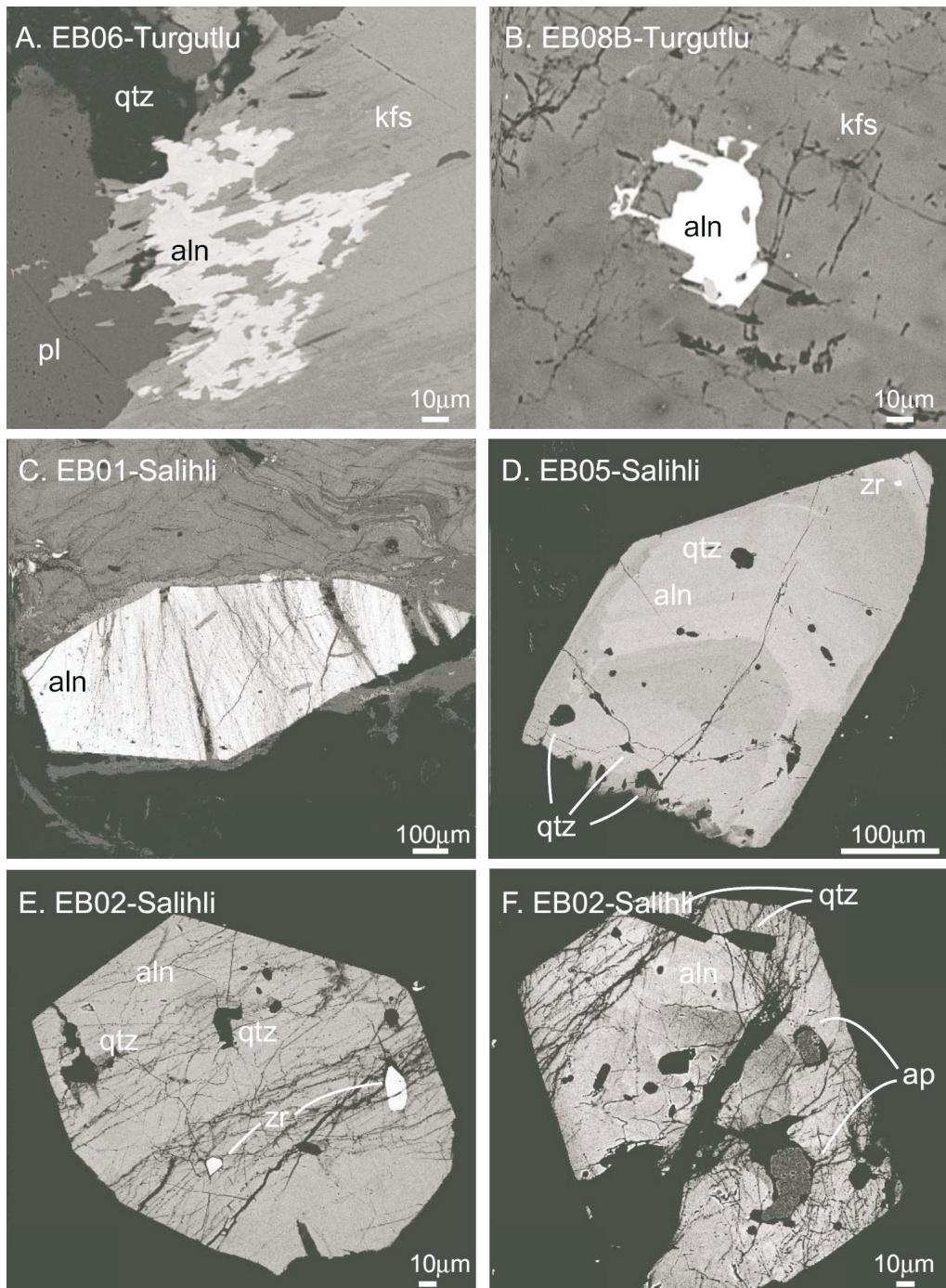


Fig. 5. Backscattered electron (BSE) images of allanite grains in Turgutlu (A–B) and Salihli samples (C–F). Sample numbers are indicated. Abbreviations after Kretz (1983)

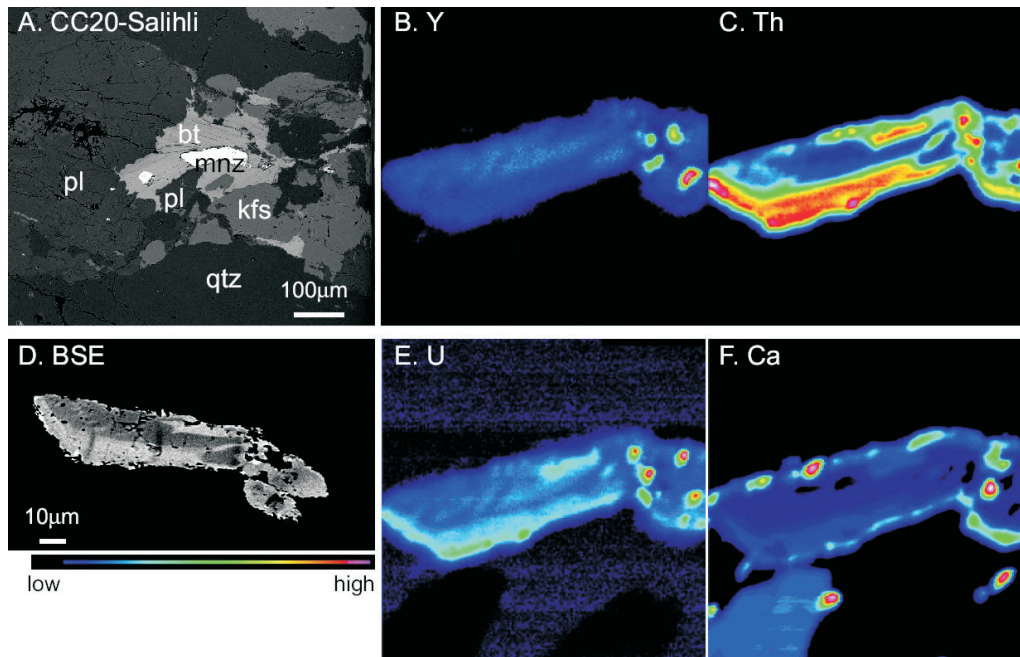


Fig. 6. BSE images and X-ray element maps of a monazite grain in Salihli granite sample CC20

Alasehir detachment granites display a range of SiO_2 contents that range from 65.25 wt% (our data; Table 2) to 77.16 wt% (Glodny and Hetzel 2007), and show roughly linear trends in major element- SiO_2 variation diagrams. Their CaO, MgO, Fe_2O_3 (total), MnO, Al_2O_3 , TiO_2 , and P_2O_5 wt% decrease with increasing SiO_2 contents, whereas their Na_2O and K_2O wt% are scattered, but generally increase. The Turkish granites with allanite are characterized by higher Ca, as evidenced in a R1 $[4\text{Si}-11(\text{Na}+\text{K})-2(\text{Fe}+\text{Ti})]$ vs. R2 $[6\text{Ca}+2\text{Mg}+\text{Al}]$ diagram (De la Roche 1980) (Fig. 9). Compared with rocks with monazite only, granites from Turkey with allanite only contain higher CaO (4.00 ± 0.30 wt% vs. 0.95 ± 0.41 wt%) and higher Al_2O_3 (16.0 ± 0.4 wt% vs. 14.1 ± 1.1 wt%; Fig. 9). Monazite can persist at higher Ca and Al contents, as illustrated by sample EB06, which contains both monazite and allanite and has 3.75 wt% CaO and 15.96 wt% Al_2O_3 (Table 3). This rock is compositionally similar to EB01 and EB05, which both contain allanite only. Monazite grains in EB06 are small (~ 10 – 50 μm) and are either rounded or are part of reaction textures in contact with apatite and huttonite (Fig. 10).

The generalization that monazite and/or allanite will crystallize at a certain Ca activity for all granitic lithologies is not valid. For example, we compare our dataset to A-type granites exposed in eastern China (Fig. 9; Wu et al. 2002; Qiu et al. 2004; Xie et al. 2006). These A-type granites show an opposite relationship to the Turkish samples in a R1 vs. R2 diagram, with allanite found in rocks with lower R2 values than those with monazite only (258 ± 29 vs. 301 ± 26 ; Fig. 9). The peralkaline A-type granites with allanite from SE China average 0.5 ± 0.2 wt% CaO, whereas aluminous granites with monazite average 0.6 ± 0.2 wt% (Qiu et al. 2004). Monazite may be present in S-type granites with higher CaO contents, but no correlation is found in A-type lithologies.

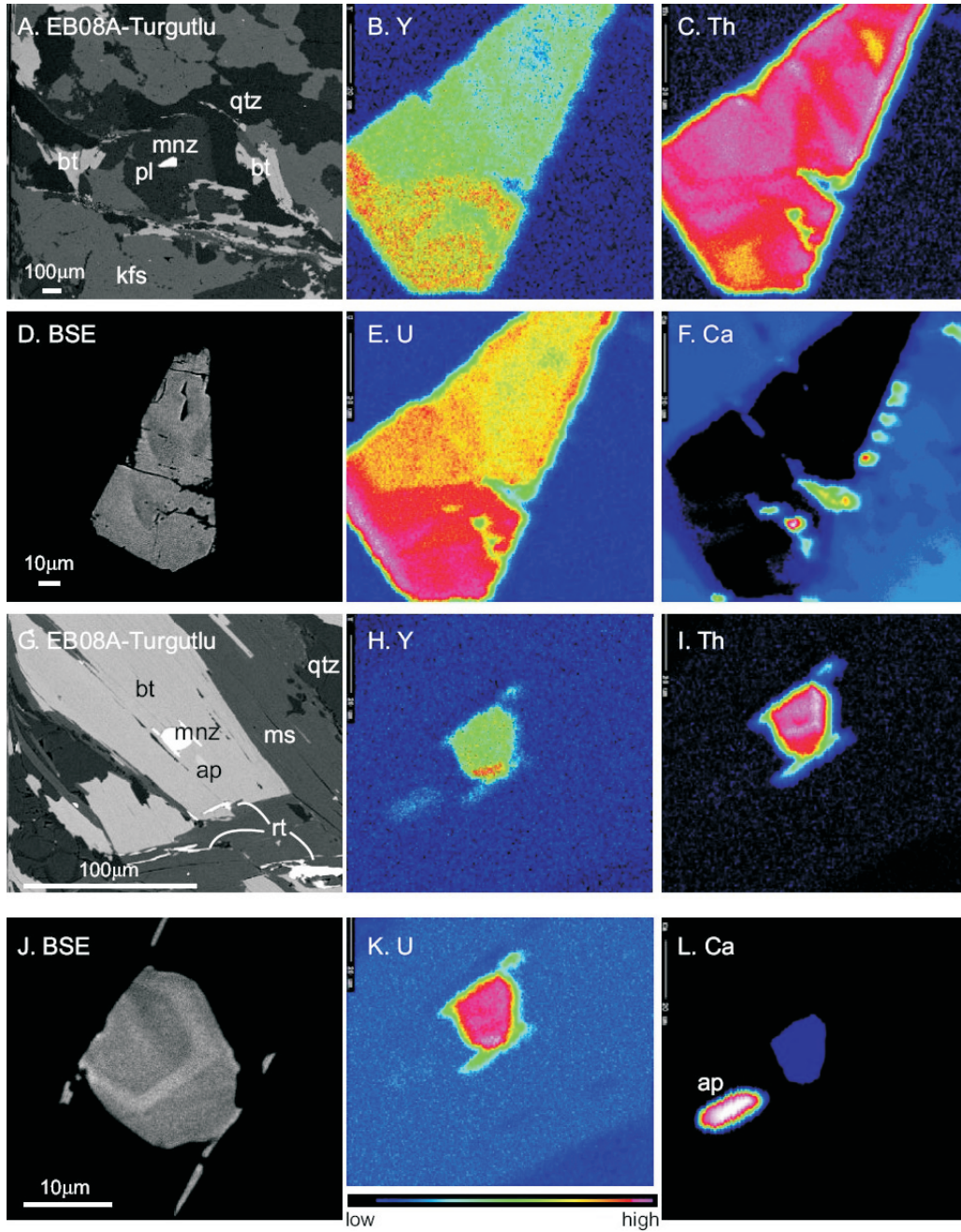


Fig. 7. BSE images and X-ray element maps of two monazite grains in Turgutlu granite sample EB08A

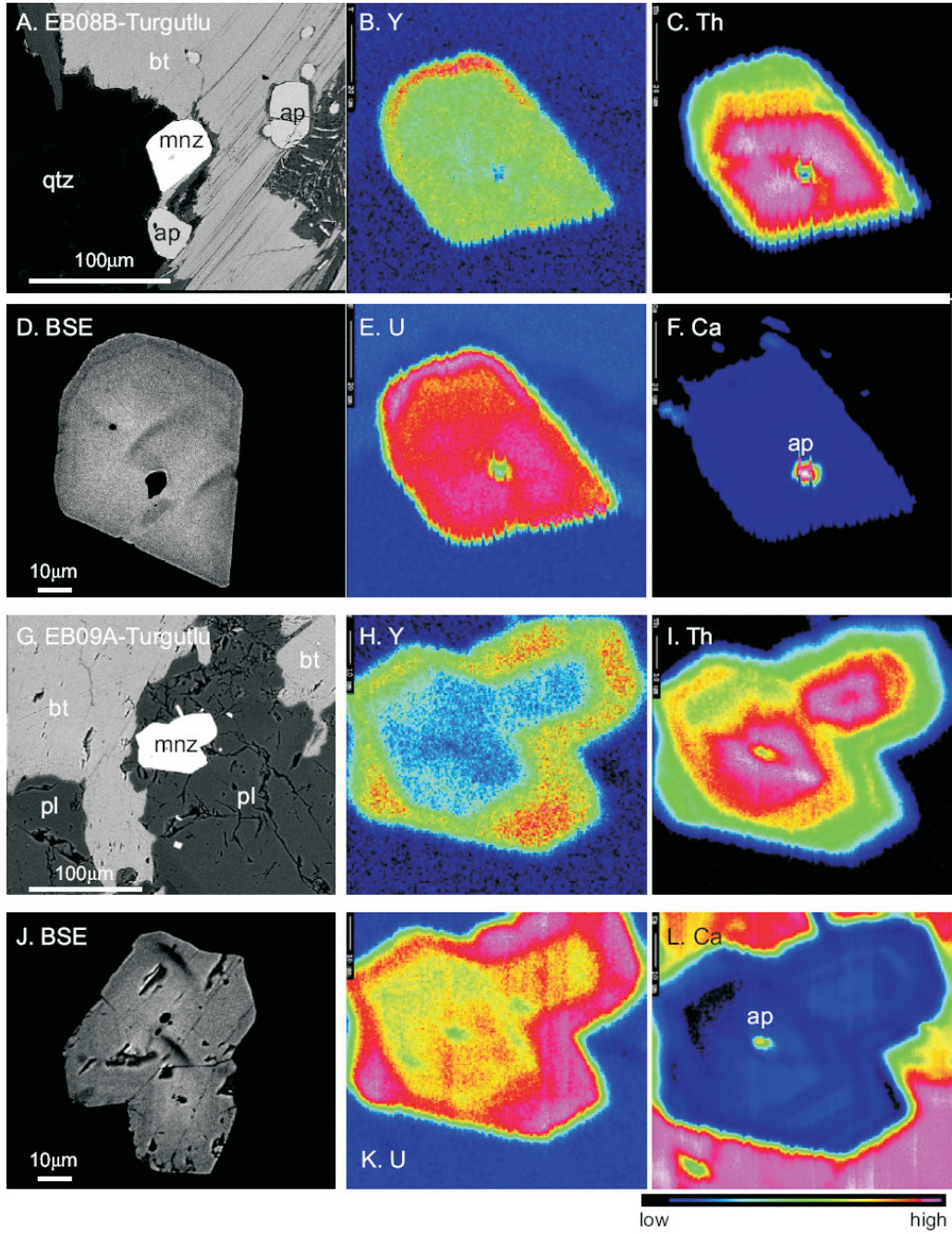


Fig. 8. BSE images and X-ray element maps of two monazite grains in Turgutlu granite sample EB08B (A–F) and EB09A (G–L)

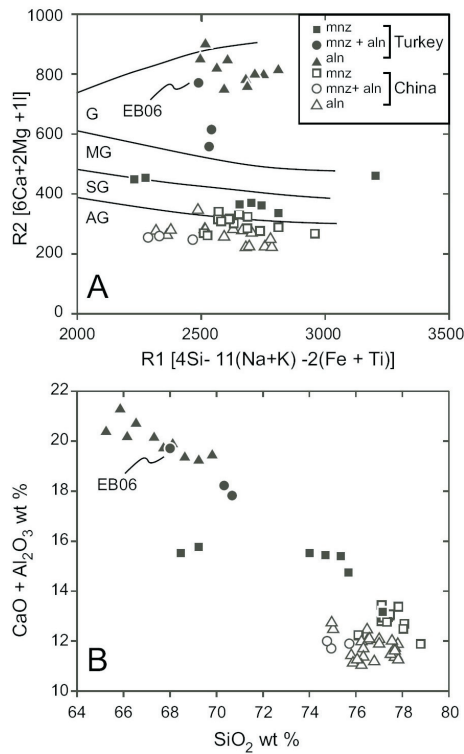


Fig. 9. (A) Classification of the Salihli and Turgutlu plutonic rocks (Turkey; Tables 2–3 and analyses from Glodny and Hetzel 2007) using parameters R1 and R2 (after de La Roche 1980). G = granodiorites, MG = monzogranite, SG = syenogranite, AG = alkali granite fields. Also included are compositional analyses of A-type granites from China (Wu et al. 2002; Qiu et al. 2004; Xie et al. 2006). (B) SiO₂ vs. CaO+Al₂O₃ wt% for granites from Turkey and China. Symbols and data set are the same as those indicated in (A). Sample EB06 is indicated for reference

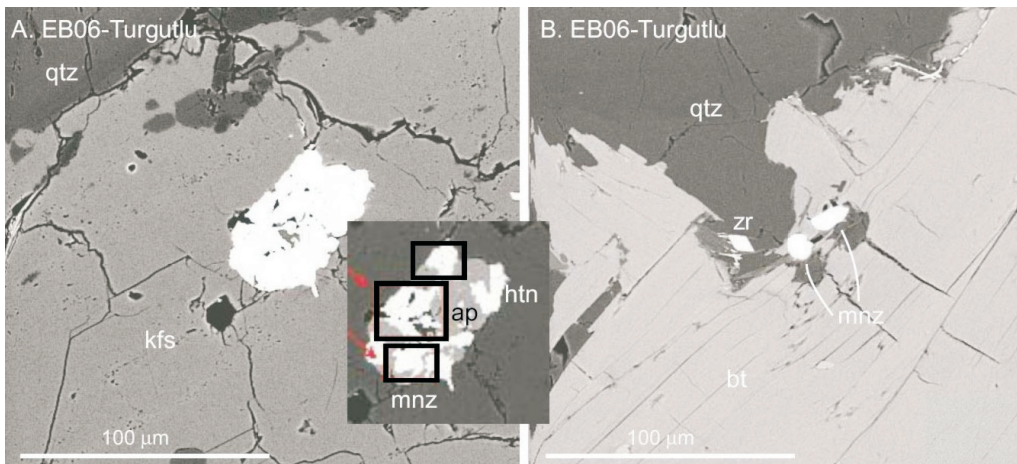


Fig. 10. BSE images of monazite from Turgutlu granite sample EB06. Inset shows a high contrast BSE image of the grain in (A)

The debate regarding bulk chemical control on the presence of monazite and/or allanite in metamorphic rocks has been ongoing (e.g., Fitzsimons et al. 2005; Rasmussen et al. 2006). Ca and Al activities are invoked to control the crystallization of monazite at the biotite isograd (e.g., Wing et al. 2003). Compositionally identical assemblages will contain either monazite or allanite depending on metamorphic grade (Smith and Barreiro 1990; Kingsbury et al. 1993). However, monazite could crystallize at significantly different times (as much as >100 m.y. apart) in rocks that experience similar metamorphic conditions, but differ in Fe and Mg contents (Fitzsimons et al. 2005). Some find no correlation between the presence of metamorphic monazite and whole rock compositions (e.g., Rubatto et al. 2001). The assumption that the presence of monazite in a pelitic schist may be solely related to a rock's bulk composition during metamorphism has significant implications for those seeking to use the mineral to time tectonic events (see Rasmussen et al. 2006).

To address this issue, we obtained geochemical information from garnet-bearing Bayindir and Bozdag nappe rocks from western Turkey (Table 1 and 4). Some samples (MM40, MM39, and MM36) contain allanite coexisting with monazite (Table 1; Fig. 11), suggested to be rare (Krenn and Finger 2007). In Menderes Massif rocks, allanite is commonly observed in contact with monazite (Fig. 11; see also Catlos and Çemen 2005).

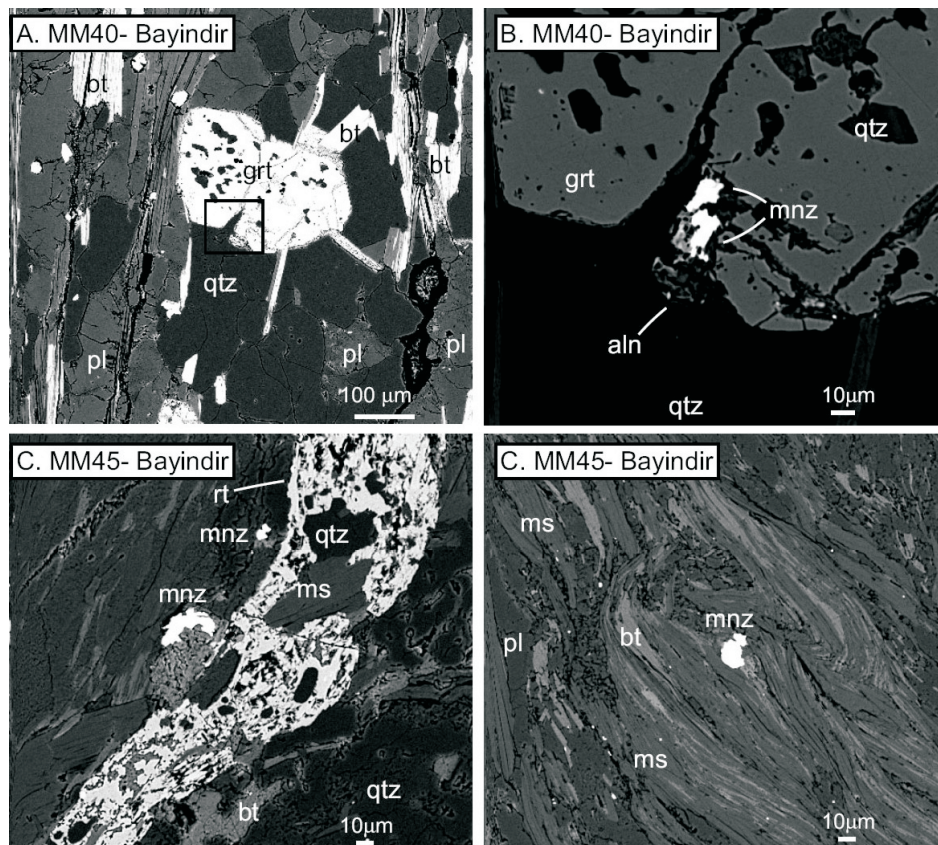


Fig. 11. BSE images of monazite grains from Bayindir nappe samples MM40 (A–B) and MM45 (C–D)

Using the geochemical data alone, no assumptions can be made about the presence of monazite or allanite in the metamorphic rocks analyzed in this study (Fig. 12). For example, the idea that higher CaO content stabilizes allanite at the expense of monazite is incorrect, as sample MM45 contains monazite and has ~7.04 wt% CaO. Monazite in MM45 are small (10–30 μm -sized) anhedral grains that have a frayed edges and irregular boundaries. The large amount of Ca present in this sample suggests the rock may have been subjected to fluid interaction and alteration, an idea supported by petrographic observations and BSE images (Fig. 11).

The Bayindir rocks likely experienced a range of P-T conditions and may have been metamorphosed more than once. For example, sample MM48 contains garnets of varying size, with larger subhedral garnets in mica-rich layers and smaller euhedral garnets in the coarse-grained quartz veins (Fig. 13). Compositional traverses were made from rim to rim across two garnets in this rock. The larger subhedral garnet shows characteristic prograde zoning, with a bell-shaped zoning profile in spessartine that decreases from 0.059 mole fraction in the core to 0.006 mole fraction at the outermost rim. Fe/(Fe+Mg) decreases from 0.905 in the core to 0.864 at the rim, consistent with growth under increasing T. Grossular content is flat (0.154 ± 0.011 mole fraction) and pyrope steadily increases from core to rim (from 0.074 mole fraction to 0.114). These observations sharply contrast with the zoning profiles of a smaller, euhedral garnet located <9 mm away in the same thin section. This garnet shows characteristic retrograde zoning, with a u-shaped zoning profile in spessartine that increases from 0.016 ± 0.007 mole fraction in the core to 0.036 mole fraction at the outermost rim. In this garnet, Fe/(Fe+Mg) increases from core to rim (from 0.829 to 0.901). Both grossular and pyrope sharply decrease at the rims (e.g., from 0.090 to 0.062 mole fraction grossular and from 0.139 to 0.090 mole fraction pyrope). We speculate the garnets MM48 formed during different tectonic events and through different reaction histories.

The metamorphic assemblages from the Menderes Massif demonstrate that no correlation exists between the presence or absence of monazite and whole rock major element compositions.

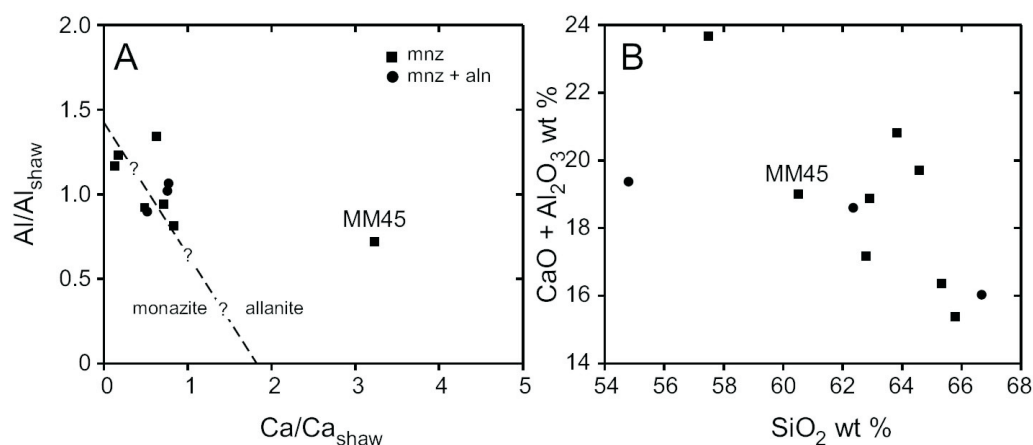


Fig. 12. (A) Whole rock Ca and Al contents of pelitic schists from the Bayindir and Bozdag nappes of western Turkey. Values referenced to Shaw's average pelite (Shaw 1956) after Wing et al. (2003). Dashed line is the inferred control line of whole-rock composition on the formation of allanite at the biotite isograd. (B) SiO₂ vs. CaO+Al₂O₃ wt% for Bayindir and Bozdag metamorphic assemblages. Sample MM45 is indicated for reference

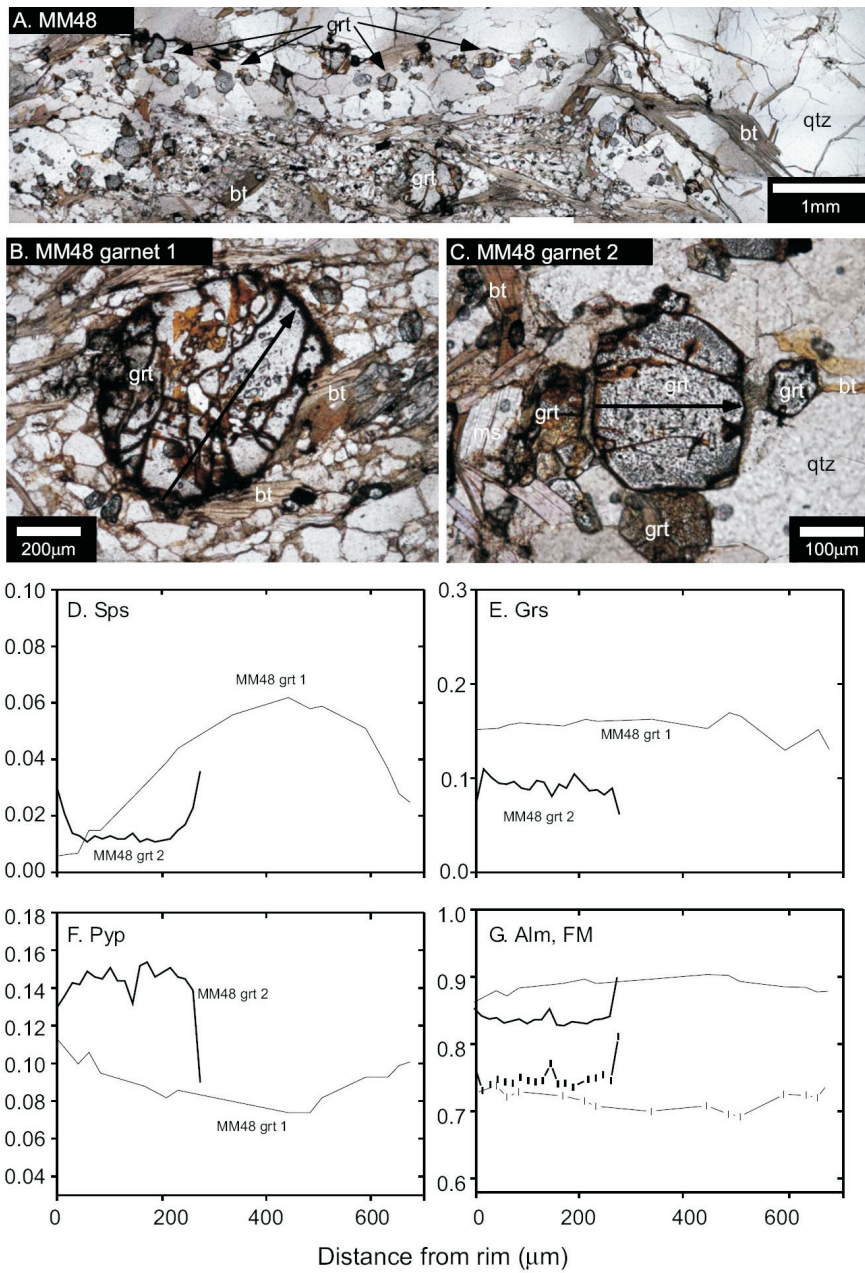


Fig. 13. (A–C) Petrographic images of garnets in sample MM48. Scale bar is indicated. Arrows on (B) and (C) indicate the path of the compositional traverses plotted below. The arrowheads indicate the end point. The figure also includes compositional traverse from rim to core to rim across two garnets in samples MM048 in (C) Sps = spessartine, (D) Grs = grossular, (E) Pyp = pyrope, and (F) Alm = almandine and FM = Fe/(Fe+Mg). The larger garnet was located <9 mm away from the smaller grain. Tick marks are plotted on the almandine traverses; the each tick corresponds to the location of an analysis. The length of the tick has no statistical significance

The presence of monazite in a metamorphic rock can be influenced by the number, duration, and type of metamorphic events that were experienced, as well as the degree to which fluids were involved. Monazite in some of the Bayindir and Bozdag samples are commonly seen in contact with allanite (Fig. 11; Catlos and Çemen 2005), indicating that the source of monazite in these rocks was likely reactions that involved allanite. These reactions may not have significantly changed the rock's bulk composition.

5. Discussion

Geochemical and petrological analyses of igneous and metamorphic assemblages from western Turkey indicate that whole rock composition alone cannot delineate the presence of monazite and/or allanite. Monazite is present in S-type Menderes Massif granites at lower CaO and Al₂O₃ contents, a trend consistent with the observations of numerous researchers. However, applying this generalization to all granites is invalid, as A-type granites do not show the same relationship (Fig. 9). The presence of monazite in granitic rocks is likely influenced by factors that distinguish S- and A-type granites, such as the magma differentiation path, temperature of melt, and/or tectonic setting. The correlation seen in S-type granites with Ca and Al contents and monazite stability may be the result, rather than the control, disguising the true nature of other important influences that create monazite in igneous lithologies. Ca-rich phases (e.g., apatite) are present in Menderes Massif S-type granites that contain monazite (Figs. 7 and 8). Monazite grains that were element mapped show increases in Ca at rims and in cracks (Figs. 6 and 7), suggesting the possible presence of Ca-rich fluids that may act to trigger dissolution/reprecipitation reactions.

Monazite may form a variety of reactants (see Catlos et al. 2002 for a review; Kohn and Malloy 2004) and under different P-T conditions, depending on mineral assemblage, duration of metamorphism, presence or absence of fluids, and available reactants. Sample MM48 illustrates the complicated tectonic history experienced by the metamorphic assemblages of the Menderes Massif, as it contains garnets of opposite zoning. The events that transpired to create this rock would likely be represented by monazite present in the sample. However, this rock's whole rock composition is not especially useful for understanding its geologic history.

We suggest that prior to interpreting any monazite age, assumptions must be made regarding (1) the reactant that formed the monazite grain, (2) a rock's cooling or P-T history, (3) peak P-T conditions, (4) tectonic environment, (5) duration of metamorphism, and (6) interaction with fluids. Knowledge about the timing of events (diagenetic, tectonic, magmatic) occurring elsewhere and relying on other geochronologic constraints (apatite fission track, ⁴⁰Ar/³⁹Ar geochronology, U-Pb zircon ages) are required. In situ techniques to chemically analyze and date monazite (i.e., electron microprobe, ion microprobe) facilitate understanding of the geochronologic results. Considerable insight can be made regarding the rates and mechanisms of plate tectonics using monazite as a geochronometer. However, the mineral's presence in igneous and metamorphic rocks is not controlled solely by major element chemistry.

Acknowledgements. This work was supported by an award to Drs. E.J. Catlos, I. Çemen, and M.J. Kohn from the U.S. National Science Foundation (NSF-0440169). CC and EB samples were collected with assistance from Drs. M.J. Kohn

and M. Cemal Göncüoğlu. MM samples were collected with assistance from Halil Kahraman and the people in Horzumalayaka village. Rock samples were analyzed for their major element chemistry by Activation Laboratories. Electron microprobe analyses were obtained at Oklahoma State University (Boone Pickens School of Geology) and University of Texas at Austin (Jackson School of Geosciences). We greatly appreciate the constructive reviews of the editor, Dr. Andrzej Skowronski, and two anonymous reviewers.

6. References

- AKERS W.T., GROVE M., HARRISON T.M., RYERSON F.J., 1993: The instability of rhabdophane and its unimportance in monazite paragenesis. *Chemical Geology* 110, 169–176.
- BARAKAT M.A., HAMED H.A., KHOLIEF M.M., 1993: Mineralogical studies on subsurface Jurassic and Lower Cretaceous sandstones from the western desert, Egypt. *Journal of Petroleum Geology* 16, 213–222.
- BINGEN B., DEMAIFFE D., HERTOGEN J., 1996: Redistribution of rare earth elements, thorium, and uranium over accessory minerals in the course of amphibolite to granulite facies metamorphism: the role of apatite and monazite in orthogneisses from southwestern Norway. *Geochimica et Cosmochimica Acta* 60, 1341–1354.
- BOZKURT E., OBERHAENSLI R., 2001: Menderes Massif (western Turkey): Structural, metamorphic and magmatic evolution: A synthesis. *International Journal of Earth Sciences* 89, 679–708.
- BROSKA I., PETRIK I., WILLIAMS C.T., 2000: Coexisting monazite and allanite in peraluminous granitoids of the Tribec Mountains, Western Carpathians. *American Mineralogist* 85, 22–32.
- BROSKA I., SIMAN P., 1998: The breakdown of monazite in the West-Carpathian Veporic orthogneisses and Tatric granites. *Geologica Carpathica Bratislava* 49, 161–167.
- BRUHN F., MOLLER A., SIE S.H., HENSEN B.J., 1999: U-Th-Pb chemical dating of monazites using the proton microprobe. *Nuclear Instruments and Methods in Physics Research B: Beam Interactions with Materials and Atoms*, 158, 616–620.
- CATLOS E.J., ÇEMEN I., 2005: Monazite ages and the evolution of the Menderes Massif. *International Journal of Earth Sciences* 94, 204–217.
- CATLOS E.J., GILLEY L.D., HARRISON T.M., 2002: Interpretation of monazite ages obtained via in situ analysis. *Chemical Geology* 188, 193–215.
- CATLOS E.J., HARRISON T.M., KOHN M.J., GROVE M., RYERSON F.J., MANNING C.E., UPRETI B.N., 2001: Geochronologic and thermobarometric constraints on the evolution of the Main Central Thrust, central Nepal Himalaya. *Journal of Geophysical Research-Solid Earth* 106, 16177–16204.
- ÇEMEN I., CATLOS E.J., GOGUS O., OZERDEM C., 2006: Post-Collisional Extensional Tectonics and Exhumation of the Menderes Massif in the Western Anatolia Extended Terrane, Turkey. In: Y. Dilek and S. Pavlides (eds), Post-collisional Tectonics and Magmatism in the Eastern Mediterranean Region. *Geological Society of America's Special Paper* 409, 353–379.
- CHEN C.H., LU H.Y., LIN W., LEE C.Y., 2006: Thermal event records in SE China coastal areas: Constraints from monazite ages of beach sands from two sides of the Taiwan strait. *Chemical Geology* 231, 118–134.
- CLAESSON S., BOGDANOVA S.V., BIBIKOVA E.V., GORBATSCHEV R., 2001: Isotopic evidence for Palaeoproterozoic accretion in the basement of the East European Craton. *Tectonophysics* 339, 1–18.
- CONCEICAO R., 2000: The Santanapolis Syenite; genesis and evolution of Paleoproterozoic shoshonitic syenites in the northeastern Brazil. *International Geology Review* 10, 941–957.
- CUNEY M., FRIEDRICH M., 1987: Physicochemical and crystal-chemical controls on accessory mineral paragenesis in granitoids: Implications for uranium metallogenesis. *Bulletin de Mineralogie* 110, 235–247.
- DAHL P.S., HAMILTON M.A., JERCINOVIC M.J., TERRY M.P., WILLIAMS M.L., FREI R., 2005: Comparative isotopic and chemical geochronometry of monazite, with implications for U-Th-Pb dating by electron microprobe; an example from metamorphic rocks of the eastern Wyoming Craton (U.S.A.) *American Mineralogist* 90, 619–638.
- DE LA ROCHE H., LETERRIER J., GRANDE CLAUDE P., MARCHAL M., 1980: A classification of volcanic and plutonic rocks using R1 and R2 diagrams and major element analyses: Its relationship to and current nomenclature. *Chemical Geology* 29, 183–210.

- DE MOURA J.C., WALLFASS C.M., BOSSEW P., 2002: Health hazards of radioactive sands along the coast of Espirito Santo/Brazil. *Neues Jahrbuch für Geologie und Palaontologie-Abhandlungen* 225, 127–136.
- DEWOLF C.P., BELSHAW N., ONIONS R.K., 1993: A metamorphic history from micron scale $^{207}\text{Pb}/^{206}\text{Pb}$ chronometry of Archean monazite. *Earth and Planetary Science Letters* 120, 207–220.
- DORA O.O., CANDAN O., KAYA O., KORALAY E., DURR S., 2001: Revision of “leptite-gneisses” in the Menderes Massif: A supracrustal metasedimentary origin. *International Journal of Earth Sciences* 89, 836–851.
- DOSTAL J., CHATTERJEE A.K., KONTAK D.J., 2004: Chemical and isotopic (Pb, Sr) zonation in a peraluminous granite pluton: role of fluid fractionation. *Contributions to Mineralogy and Petrology* 147, 74–90.
- EVANS J.A., CHISHOLM J.I., LENG M.J., 2001: How U-Pb detrital monazite ages contribute to the interpretation of the Pennine Basin infill. *Journal of the Geological Society* 158, 741–744.
- EVANS J., ZALASIEWICZ J., 1996: U-Pb, Pb-Pb and Sm-Nd dating of authigenic monazite; implications for the diagenetic evolution of the Welsh Basin. *Earth and Planetary Science Letters* 144, 421–433.
- EVANS J.A., ZALASIEWICZ J.A., FLETCHER I., RASMUSSEN B., PEARCE N.J.G., 2002: Dating diagenetic monazite in mudrocks: constraining the oil window? *Journal of the Geological Society* 159, 619–622.
- FINGER F., BROSKA I., 1999: The Gemic S-type granites in southeastern Slovakia: Late Palaeozoic or Alpine intrusions? Evidence from electron-microprobe dating of monazite. *Schweizerische Mineralogische und Petrographische Mitteilungen* 79, 439–443.
- FINGER F., BROSKA I., HAUNSCHMID B., HRASKO L., KOHUT M., KRENN E., PETRIK I., RIEGLER G., UHER P., 2003: Electron-microprobe dating of monazites from Western Carpathian basement granitoids: plutonic evidence for an important Permian rifting event subsequent to Variscan crustal anatexis. *International Journal of Earth Sciences* 92, 86–98.
- FITZSIMONS I.C.W., KINNY P.D., WETHERLEY S., HOLLINGSWORTH, D.A., 2005: Bulk chemical control on metamorphic monazite growth in pelitic schists and implications for U-Pb age data. *Journal of Metamorphic Geology* 23, 261–277.
- GESSNER K., COLLINS A.S., RING U., GUNGOR T., 2004: Structural and thermal history of poly-orogenic basement: U-Pb geochronology of granitoid rocks in the southern Menderes Massif, Western Turkey. *Journal of Geological Society* 161, 93–101.
- GESSNER K., RING U., PASSCHIER C.W., JOHNSON C., HETZEL R., GUNGOR T., 2001: An active bivergent rolling-hinge detachment system: Central Menderes metamorphic core complex in western Turkey. *Geology* 29, 611–614.
- GILLEY L.D., HARRISON T.M., LELOUP P.H., RYERSON F.J., LOVERA O.M., WANG J.H., 2003: Direct dating of left-lateral deformation along the Red River shear zone, China and Vietnam. *Journal of Geophysical Research-Solid Earth* 108, Art. No. 2127.
- GILOTTI J.A., MCCLELLAND, W.C., 2005: Leucogranites and the time of extension in the East Greenland Caledonides. *Journal of Geology* 113, 399–417.
- GLODNY J., HETZEL, R., 2007: Precise U-Pb ages of syn-extensional Miocene intrusions in the central Menderes Massif, western Turkey. *Geological Magazine* 144, 235–246.
- GONZÁLEZ-ÁLVAREZ I., KUSIAK M.A., KERRICH R., 2006: A trace element and chemical Th-U total Pb dating study in the lower Belt-Purcell Supergroup, Western North America: Provenance and diagenetic implications. *Chemical Geology* 230, 140–160.
- GROVE M., HARRISON T.M. 1999: Monazite Th-Pb age depth profiling. *Geology* 27, 487–490.
- HARRISON T.M., GROVE M., LOVERA O.M., CATLOS E.J., 1998: A model for the origin of Himalayan anatexis and inverted metamorphism. *Journal of Geophysical Research-Solid Earth* 103, 27017–27032.
- HARRISON T.M., MCKEEGAN K.D., LEFORT P., 1995: Detection of inherited monazite in the Manaslu leucogranite by $^{208}\text{Pb}/^{232}\text{Th}$ ion microprobe dating: Crystallization age and tectonic implications. *Earth and Planetary Science Letters* 133, 271–282.
- HARRISON T.M., RYERSON F.J., LEFORT P., YIN A., LOVERA O.M., CATLOS E.J., 1997: A Late Miocene-Pliocene origin for the Central Himalayan inverted metamorphism. *Earth and Planetary Science Letters* 146, E1–E7.
- HERMANN J., RUBATTO D., 2003: Relating zircon and monazite domains to garnet growth zones: age and duration of granulite facies metamorphism in the Val Malenco lower crust. *Journal of Metamorphic Geology* 21, 833–852.

- HETZEL R., PASSCHIER C.W., RING U., and DORA, O.O., 1995b: Bivergent extension in orogenic belts; the Menderes Massif (southwestern Turkey). *Geology* 23, 455–458.
- HETZEL R., RING U., AKAL C., and TROESCH M., 1995a: Miocene NNE-directed extensional unroofing in the Menderes Massif, southwestern Turkey. *Journal of Geological Society of London* 152, 639–654.
- HLAVA P.F., 1974: Unusual lavas from Molokai, Hawaii; alkalic olivine basalts transitional to hawaiites and strontium-rich mugearites. University of New Mexico : Albuquerque, NM, United States; Master's Thesis, 170 p.
- ISIK V., SEYITOGLU G., and CEMEN I., 2003: Ductile-brittle transition along the Alasehir detachment fault and its structural relationship with the Simav detachment fault, Menderes massif, western Turkey. *Tectonophysics* 374, 1–18.
- JANOTS E., BRUNET F., GOFFÉ B., POINSSOT C., BURCHARD M., and CEMIČ L., 2007: Thermochemistry of monazite-(La) and dissakisite-(La): implications for monazite and allanite stability in metapelites. *Contributions to Mineralogy and Petrology*, 154, 1–14.
- JAIKRISHAN G., ANDREWS V.J., THAMPI M.V., KOYA P.K.M., RAJAN V.K., CHAUHAN P.S., 1999: Genetic monitoring of the human population from high-level natural radiation areas of Kerala on the southwest coast of India. I. Prevalence of congenital malformations in newborns. *Radiation Research* 152, S149–S153.
- JERCINOVIC M.J., WILLIAMS M.L., 2005: Analytical perils (and progress) in electron microprobe trace element analysis applied to geochronology; background acquisition, interferences, and beam irradiation effects. *American Mineralogist*, 90, 526–546.
- KANAZAWA Y., KAMITANI M., 2006: Rare earth minerals and resources in the world. *Journal of Alloys and Compounds* 408, 1339–1343.
- KAPOOR S.S., RAMAMURTHY V.S., LAL M., KATARIA S.K., 1977: Search for superheavy elements in monazite from beach sands of South India. *Pramana* 9, 515–521.
- KARTASHOV P.M., BOGATIKOV O.A., MOKHOV A.V., GORSHKOV A.I., ASHIKHMINA N.A., MAGAZINA L.O., KOPORULINA E.V., 2006: Lunar monazites. *Doklady Earth Sciences* 407, 498–502.
- KAUR P., CHAUDHRI N., BIJU-SEKHAR S., YOKOYAMA K., 2006: Electron probe micro analyser chemical zircon ages of the Khetri granitoids, Rajasthan, India: Records of widespread late palaeoproterozoic extension-related magmatism. *Current Science* 90, 65–73.
- KIM S.J., LEE H.K., YIN J.W., PARK J.K., 2005: Chemistry and origin of monazites from carbonatite dikes in the Hongcheon-Jaeun district, Korea. *Journal of Asian Earth Sciences* 25, 57–67.
- KINGSBURY J.A., MILLER C.F., WOODEN J.L., and HARRISON T.M., 1993: Monazite paragenesis and U-Pb systematics in rocks of the eastern Mojave Desert, California, U.S.A.: implications for thermochronometry. *Chemical Geology* 110, 147–167.
- KOHN M.J., MALLOY, M.A., 2004: Formation of monazite via prograde metamorphic reactions among common silicates; implications for age determinations. *Geochimica et Cosmochimica Acta* 68, 101–113.
- KONAK N., 2002, The Geological Map of Turkey. General Directorate of Mineral Research and Exploration. Izmir Area Map.
- KOVALENKO V. I., TSARYEVA G.M., GOREGLYAD A.V., YARMOLYUK V.V., TROITSKY V.A., HERVIG R.L., FARMER G.L., 1995: The peralkaline granite-related Khaldzan-Buregtey rare metal (Zr, Nb, REE) deposit, western Mongolia. In: P.J. Pollard, (ed), A special issue devoted to the geology of rare metal deposits. *Economic Geology and the Bulletin of the Society of Economic Geologists* 90, 530–547.
- KRENN E., FINGER F., 2007: Formation of monazite and rhabdophane at the expense of allanite during Alpine low temperature retrogression of metapelitic basement rocks from Crete, Greece: Microprobe data and geochronological implications. *Lithos* 95, 130–147.
- KRETZ R., 1983: Symbols for rock-forming minerals. *American Mineralogist* 68, 277–279.
- KUSIAK M.A., KEDZIOR A., PASZKOWSKI M., SUZUKI K., GONZALEZ-ALVAREZ I., WAJSPRYCH B., DOKTOR M., 2006: Provenance implications of Th-U-Pb electron microprobe ages from detrital monazite in the Carboniferous Upper Silesia Coal Basin, Poland. *Lithos* 88, 56–71.
- KUSIAK M.A., LEKKI J., 2008: Proton microprobe for chemical dating of monazite. *Gondwana Research*, in press, DOI: 10.1016/j.gr.2008.01.011.
- KUSIAK M.A., SUZUKI K., DUNKLEY D.J., LEKKI J., BAKUN-CZUBAROW N., PASZKOWSKI M., BUDZYŃ B., 2008: EPMA and PIXE dating of monazite in granulites from Stary Gierałtów, NE Bohemian Massif, Poland. *Gondwana Research*, DOI: 10.1016/j.gr.2008.02.005.

- LEE D.E., DODGE F.C.W., 1964: Accessory minerals in some granitic rocks in California and Nevada as a function of calcium content. *American Mineralogist* 49, 1660–1669.
- LEKKI J., LEBED S., PASZKOWSKI M.L., KUSIAK M., VOGT J., HAJDUK R., POLAK W., POTEMPA A., STACHURA Z., STYCZEN J., 2003. Age determination of monazites using the new experimental chamber of the Cracow proton microprobe. *Nuclear Instruments and Methods in Physics Research B: Beam Interactions with Materials and Atoms*, 210, 472–477.
- LEV S.M., MCLENNAN S.M., HANSON G.N., 1999: Mineralogic controls on REE mobility during black-shale diagenesis. *Journal of Sedimentary Research* 69, 1071–1082.
- LEV S.M., MCLENNAN S.M., HANSON G.N., 2000: Late diagenetic redistribution of uranium and disturbance of the U-Pb whole rock isotope system in a black shale. *Journal of Sedimentary Research* 70, 1234–1245.
- LEV S.M., MCLENNAN S.M., MEYERS W.J., HANSON G.N., 1998: A petrographic approach for evaluating trace-element mobility in a black shale. *Journal of Sedimentary Research* 68, 970–980.
- LISITSINA G.A., BOGDANOVA V.I., VARSHAL G.M., SIROTININA N.A., 1965: Geochemistry of accessory minerals in the Charkasar granites of the Kuraminskiy range (Tien Shan). *Geochemistry International* 2, 463–475.
- LOOS S., REISCHMANN T., 1999: The evolution of the southern Menderes Massif in SW Turkey as revealed by zircon dating. *Journal of Geological Society of London* 156, 1021–1030.
- LOVERING J.F., WARK D.A., GLEADOW A.J.W., BRITTEN R., 1974: Lunar monazite; a late-stage (mesostasis) phase in mare basalt. *Earth and Planetary Science Letters* 21, 164–168.
- MACHADON., GAUTHIER G., 1996: Determination of Pb-207/Pb-206 ages on zircon and monazite by laser-ablation ICPMS and application to a study of sedimentary provenance and metamorphism in southeastern Brazil. *Geochimica et Cosmochimica Acta* 60, 5063–5073.
- MARTIN B.W., 1980: A microprobe based on (PIXE); a powerful tool for microanalysis in minerals and cells. *Scanning Electron Microscopy* 1980, 419–438.
- MAZZOLI C., HANCHAR J.M., DELLA MEA G., DONOVAN J.J., STERN R.A., 2002: Mu-PIXE analysis of monazite for total U-Th-Pb age determination. *Nuclear Instruments and Methods in Physics Research B: Beam Interactions with Materials and Atoms*, 189, 394–399.
- MEYER F.M., ROBB L.J., REIMOLD W.U., DEBRUIYN H., 1994: Contrasting low-Ca and high-Ca granites in the Archean Barberton Mountain Land, Southern Africa. *Lithos* 32, 63–76.
- MILLIKEN K.L., 2007: Provenance and diagenesis of heavy minerals, Cenozoic units of the Northwester Gulf of Mexico sedimentary basin. *Developments in Sedimentology* 58, 247–261.
- MONTEL J.M., FORET S., VESCHAMBRE M., NICOLLET C., PROVOST A., 1996: Electron microprobe dating of monazite. *Chemical Geology* 131, 37–53.
- MONTERO P., FLOOR P., CORRETGE G., 1988: The accumulation of rare-earth and high-field-strength elements in peralkaline granitic rocks: The Galineiro orthogneiss complex, northwestern Spain. *Canadian Mineralogist* 36, 683–700.
- MORTON A.C., HALLSWORTH C., 1994: Identifying provenance-specific features of detrital heavy mineral assemblages in sandstones. *Sedimentary Geology* 90, 241–256.
- MURPHY M.A., COPELAND P., 2005: Transtensional deformation in the central Himalaya and its role in accommodating growth of the Himalayan orogen. *Tectonics* 24, Art. No. TC4012.
- ÖRGÜN Y., ALTINSOY N., ŞAHİN S.Y., GÜNGÖR Y., GÜLTEKİN A.H., KARAHAN G., KARACIK, Z., 2007: Natural and anthropogenic radionuclides in rocks and beach sands from Ezine region (Canakkale), Western Anatolia, Turkey. *Applied Radiation and Isotopes* 65, 739–747.
- OVERSTREET W.C., 1967: The geologic occurrence of monazite. *Geological Survey Professional Papers* 530, 1–327.
- PARRISH, R.R., 1990: U-Pb dating of monazite and its application to geological problems. *Canadian Journal of Earth Sciences* 27, 1431–1450.
- POITRASSON F., CHENERY S., BLAND D.J., 1996: Contrasted monazite hydrothermal alteration mechanisms and their geochemical implications. *Earth and Planetary Science Letters* 145, 79–96.
- PYLE J.M., SPEAR F.S., WARK D.A., DANIEL C.G., STORM L.C., 2005. Contributions to precision and accuracy of monazite microprobe ages. *American Mineralogist*, 90, 547–577.

- QIU J.S., WANG D.Z., MCINNES B.I.A., JIANG S.Y., WANG R.C., KANISAWA, S., 2004: Two subgroups of A-type granites in the coastal area of Zhejiang and Fujian Provinces, SE China: age and geochemical constraints on their petrogenesis. *Transactions of the Royal Society of Edinburgh- Earth Sciences* 95, 227–236.
- RASMUSSEN B., FLETCHER I.R., MUHLING J.R., 2007: In situ U-Pb dating and element mapping of three generations of monazite: Unravelling cryptic tectonothermal events in low-grade terranes. *Geochimica et Cosmochimica Acta* 71, 670–690.
- RASMUSSEN B., MUHLING J.R., FLETCHER I.R., WINGATE M.T.D., 2006: In situ SHRIMP U-Pb dating of monazite integrated with petrology and textures: Does bulk composition control whether monazite forms in low-Ca pelitic rocks during amphibolite facies metamorphism? *Geochimica et Cosmochimica Acta* 70, 3040–3058.
- REGNIER J-L., MEZGER J.E., PASSHIER C.W., 2007: Metamorphism of Precambrian-Paleozoic schists of the Menderes core series and contact relationships with Proterozoic orthogneisses of the western Cine Massif, Anatolide belt, Western Turkey. *Geological Magazine*, 144, 67–104.
- RING U., BUCHWALDT R., GESSNER K., 2004: Pb/Pb dating of garnet from the Anatolide belt in western Turkey: Regional implications and speculations on the role Anatolia played during the amalgamation of Gondwana. *Zeitschrift der Deutschen Geologischen Gesellschaft* 154, 537–555.
- RING U., WILLNER A.P., LACKMANN, W., 2001: Stacking of nappes with different pressure-temperature paths; an example from the Menderes Nappes of western Turkey. *American Journal of Science* 301, 912–944.
- RUBATTO D., WILLIAMS I.S., BUICK I.S., 2001: Zircon and monazite response to prograde metamorphism in the Reynolds Range, central Australia. *Contributions to Mineralogy and Petrology* 140, 458–468.
- SANTOSH M., COLLINS A.S., TAMASHIRO I., KOSHIMOTO S., TSUTSUMI Y., YOKOYAMA K., 2006: The timing of ultrahigh-temperature metamorphism in Southern India: U-Th-Pb electron microprobe ages from zircon and monazite in sapphirine-bearing granulites. *Gondwana Research* 10, 128–155.
- SATIR M., FRIEDRICHSEN H., 1986: The origin and evolution of the Menderes Massif, W-Turkey: A rubidium/strontium and oxygen isotope study. *International Journal of Earth Sciences* 75, 703–714.
- SCHÄRER U., ALLÈGRE C.J., 1983: The Palung granite (Himalaya): High-Resolution U-Pb systematics in zircon and monazite. *Earth and Planetary Science Letters* 63, 423–432.
- SCHÄRER U., COSCA M., STECK A., HUNZIKER J., 1996: Termination of major ductile strike-slip shear and differential cooling along the Insubric line (Central Alps): U-Pb, Rb-Sr and Ar-40/Ar-39 ages of cross-cutting pegmatites. *Earth and Planetary Science Letters* 142, 331–351.
- SCHÄRER U., ZHANG L-S., and TAPPONNIER, P., 1994: Duration of strike-slip movements in large shear zones: The Red River belt, China. *Earth and Planetary Science Letters* 126, 379–397.
- SENGUN F., CANDAN O., DORA O.O., and KORALAY, O.E., 2006: Petrography and geochemistry of paragneisses in the Cine submassif of the Menderes Massif, western Anatolia. *Turkish Journal of Earth Sciences* 15, 321–342.
- SEYITOGLU G., TEKELI O., ÇEMEN I., ŞEN S., and ISIK V., 2002: The role of the flexural rotation/rolling hinge model in the tectonic evolution of the Alaschir graben, western Turkey. *Geol. Mag.*, 139, 15–26.
- SHAW D.M. , 1956: Geochemistry of pelitic rocks. Part III. Major elements and general geochemistry. *Geological Society of America Bulletin* 67, 919–934.
- SIMONETTI A., HEAMAN L.M., CHACKO T., BANERJEE N.R., 2006: In situ petrographic thin section U-Pb dating of zircon, monazite, and titanite using laser ablation-MC-ICP-MS. *International Journal of Mass Spectrometry* 253, 87–97.
- SMITH H.A., BARREIRO B., 1990: Monazite U-Pb dating for staurolite grade metamorphism in pelitic schists. *Contributions to Mineralogy and Petrology* 105, 602–615.
- SNETSINGER, K.G., 1967: Accessory minerals in some Sierra Nevada granitic rocks as a function of calcium content. *American Mineralogist* 52, 832–842.
- SONG, T., 1999: The discovery of authigenic rare earth mineral-monazite from Precambrian sedimentary rock in Dalian area, Liaoning, China, and its significance. *Acta Sedimentologica Sinica* 17, 663–667.
- SÖZBİLİR H., 2001: Extension tectonics and the geometry of related macroscopic structures; field evidence from the Gediz detachment, western Turkey. *Turkish Journal of Earth Sciences* 10, 51–67.
- SUZUKI K., ADACHI M., TANAKA T., 1991: Middle Precambrian provenance of Jurassic sandstone in the Mino Terrane, Central Japan: Th-U-Total Pb evidence from an electron microprobe monazite study. *Sedimentary Geology* 75, 141–147.

- SUZUKI S., ARIMA M., WILLIAMS I.S., SHIRAIISHI K., KAGAMI H., 2006: Thermal history of UHT metamorphism in the Napier Complex, East Antarctica: Insights from zircon, monazite, and garnet ages. *Journal of Geology* 114, 65–84.
- TILTON G.R., NICOLAYSEN, L.O., 1957: The use of monazites for age determination. *Geochimica et Cosmochimica Acta* 11, 28–40.
- VAGGELLI G., BORGHI A., COSSIO R., FEDI M., GIUNTINI L., LOMBARDO B., MARINO A., MASSI M., OLMI F., PETRELLI M., 2006: Micro-PIXE analysis of monazite from the Dora Maira Massif, Western Italian Alps. *Microchimica Acta* 155, 305–311.
- VAVRA G., SCHALTEGGER U., 1999: Post-granulite facies monazite growth and rejuvenation during Permian to Lower Jurassic thermal and fluid events in the Ivrea Zone (Southern Alps). *Contributions to Mineralogy and Petrology* 134, 405–414.
- VILADKAR S.G., 1998: Carbonatite occurrences in Rajasthan, India. *Petrology* 6, 272–283.
- WALL F., MARIANO A.N., 1996: Rare earth minerals in carbonatites; a discussion centered on the Kangankunde Carbonatite, Malawi. In: A.P. Jones, F. Wall, C.T. Williams (eds) Rare Earth Minerals: Chemistry, origin, and ore deposits. *Chapman and Hall* 7, 193–225.
- WILBY P.R., PAGE A.A., ZALASIEWICZ J.A., MILODOWSKI A.E., WILLIAMS M., EVANS J.A., 2007: Syntectonic monazite in low-grade mudrocks: a potential geochronometer for cleavage formation? *Journal of the Geological Society* 164, 53–56.
- WILLIAMS M.L., JERCINOVIC M.J., 2002: Microprobe monazite geochronology: Putting absolute time into microstructural analysis. *Journal of Structural Geology* 24, 1013–1028.
- WILLIAMS M.L., JERCINOVIC M.J., TERRY M.P., 1999: Age mapping and dating of monazite on the electron microprobe: Deconvoluting multistage tectonic histories. *Geology* 27, 1023–1026.
- WILLIAMS M.L., JERCINOVIC M.J., HETHERINGTON C.J., 2007: Microprobe monazite geochronology: Understanding geologic processes by integrating composition and geochronology. *Annual Review of Earth and Planetary Sciences* 35, 137–175.
- WING B.A., FERRY J.M., HARRISON T.M., 2003: Prograde destruction and formation of monazite and allanite during contact and regional metamorphism of pelites: petrology and geochronology. *Contributions to Mineralogy and Petrology* 145, 228–250.
- WU F., SUN D., LI H., JAHN B., WILDE S., 2002: A-type granites in northeastern China; age and geochemical constraints on their petrogenesis. *Chemical Geology* 187, 143–173.
- XIE L., WANG R.C., WANG D.Z., QIU J.S., 2006: A survey of accessory mineral assemblages in peralkaline and more aluminous A-type granites of the southeast coastal area of China. *Mineralogical Magazine* 70, 709–729.
- YANG S.Y., LI C.X., YOKOYAMA K., 2006: Elemental compositions and monazite age patterns of core sediments in the Changjiang Delta: Implications for sediment provenance and development history of the Changjiang River. *Earth and Planetary Science Letters* 245, 762–776.